

Coupling of microtubule motors with AP-3 generated organelles in axons by NEEP21 family member calcyon

Liang Shi^a, Timothy Hines^b, Clare Bergson^{a,†,*}, and Deanna Smith^{b,†,*}

^aDepartment of Pharmacology and Toxicology, Medical College of Georgia, Augusta University, Augusta, GA 30912;

^bDepartment of Biological Sciences, University of South Carolina, Columbia, SC 29208

ABSTRACT Transport of late endosomes and lysosome-related organelles (LE/LROs) in axons is essential for supplying synaptic cargoes and for removing damaged macromolecules. Defects in this system are implicated in a range of human neurodegenerative and neurodevelopmental disorders. The findings reported here identify a novel mechanism regulating LE/LRO transport based on the coordinated coupling of microtubule motors and vesicle coat proteins to the neuron-enriched, transmembrane protein calcyon (Caly). We found that the cytoplasmic C-terminus of Caly pulled down proteins involved in microtubule-dependent transport (DIC, KIF5A, p150Glued, Lis1) and organelle biogenesis (AP-1 and AP-3) from the brain. In addition, RNA interference-mediated knockdown of Caly increased the percentage of static LE/LROs labeled by LysoTracker in cultured dorsal root ganglion axons. In contrast, overexpression of Caly stimulated movement of organelles positive for LysoTracker or the AP-3 cargo GFP-PI4KII α . However, a Caly mutant (ATEA) that does not bind AP-3 was unable to pull down motor proteins from brain, and expression of the ATEA mutant failed to increase either LE/LRO flux or levels of associated dynein. Taken together, these data support the hypothesis that Caly is a multifunctional scaffolding protein that regulates axonal transport of LE/LROs by coordinately interacting with motor and vesicle coat proteins.

Monitoring Editor

Jean E. Gruenberg
University of Geneva

Received: Jan 4, 2018

Revised: Apr 24, 2018

Accepted: Jun 18, 2018

INTRODUCTION

Maintaining the specialized endomembrane domains found in axons and dendrites places unique demands on cargo transport systems in neurons. Axons represent a major challenge because, in larger animals, the synapse of some motor neurons can be located meters away from the cell body. To overcome this, axonal proteins and synaptic constituents largely undergo active transport powered by cytoplasmic dynein and the kinesin family of microtubule motors

(Encalada and Goldstein, 2014). Both dynein and kinesin microtubule motor complexes use the energy of ATP hydrolysis to move associated cargoes; however, they generate forces of opposite polarity. Dynein moves cargoes retrogradely toward the cell body, whereas the kinesins move cargoes anterogradely toward growth cones and synaptic terminals. Microtubule transport is also controlled by scaffolding proteins and cargo adaptors that employ a variety of mechanisms to regulate motor activity and position (Barlan and Gelfand, 2017). Genetic defects in microtubule motors and associated proteins have been associated with a range of severe neurodegenerative and developmental disorders, including spinal muscular atrophy, Charcot-Marie-Tooth disorder, Perry syndrome, amyotrophic lateral sclerosis and lissencephaly, which underscores the importance of understanding mechanisms regulating motors in neurons (Puls *et al.*, 2003; Farrer *et al.*, 2009; Lipka *et al.*, 2013; Neveling *et al.*, 2013; Peeters *et al.*, 2013; Hoang *et al.*, 2017).

Besides moving cargoes along microtubules, dynein and kinesin play a role in the biogenesis of organelles as well as in the morphogenesis of membrane tubules (Muresan and Muresan, 2012). Membrane tubules are involved in vesicle fission and fusion; they are

This article was published online ahead of print in MBoC in Press (<http://www.molbiolcell.org/cgi/doi/10.1091/mbc.E18-01-0007>) on June 27, 2018.

[†]These authors contributed equally to the work.

*Address correspondence to: Clare Bergson (cbergson@augusta.edu) or Deanna Smith (deannasm@biol.sc.edu).

Abbreviations used: AP, adaptor protein; DIC, dynein intermediate chain; EE, early endosome; GST, glutathione-S-transferase; LE/LRO, late endosomes and lysosome-related organelles; SE, sorting endosome.

© 2018 Shi *et al.* This article is distributed by The American Society for Cell Biology under license from the author(s). Two months after publication it is available to the public under an Attribution-NonCommercial-Share Alike 3.0 Unported Creative Commons License (<http://creativecommons.org/licenses/by-nc-sa/3.0>).

"ASCB®," "The American Society for Cell Biology®," and "Molecular Biology of the Cell®" are registered trademarks of The American Society for Cell Biology.

formed on organelles as the result of a pulling force generated by motors in association with GTPases and coat proteins (Harrison *et al.*, 2003; Driskell *et al.*, 2007; Delevoye *et al.*, 2014). Heterotetrameric adaptor protein complexes AP-1 and AP-3 are among the coat proteins that have been localized to tubules (Delevoye *et al.*, 2009, 2016; Peden *et al.*, 2004). They are members of a family of cytosolic coat proteins (AP-1 to AP-5) that orchestrate the formation and sorting of vesicle carriers among the trans-Golgi network (TGN), plasma membrane, endosomes, and lysosomes (Hirst *et al.*, 2011; Bonifacino, 2014). AP-3 is the only family member with both neural specific and ubiquitous subunit isoforms (Seong *et al.*, 2005; Danglot and Galli, 2007). In neurons, AP-3 sorts synaptic vesicle (SV) and dense core vesicle (DCV) cargoes and associated presynaptic machinery from the Golgi to axons via the endolysosomal and regulated secretory pathways (Newell-Litwa *et al.*, 2007; Asensio *et al.*, 2010). AP-3 also plays a prominent role in regenerating SVs and removing proteins via late endosome and lysosomal related organelles (LE/LROs) (Salazar *et al.*, 2004; Scheuber *et al.*, 2006; Voglmaier *et al.*, 2006; Evstratova *et al.*, 2014). However, the role of microtubule motors in AP-3 cargo sorting and transport in neurons is currently poorly understood.

Recent studies suggest that the NEEP21/Caly/P19 family of neuronal and endosome-enriched transmembrane proteins could provide a possible link between AP-3 and axonal transport (Muthusamy *et al.*, 2012). One family member, NEEP21, has been proposed to contribute to axonal targeting of NgCam via a transcytotic mechanism (Yap *et al.*, 2008). In the current study, we focus on another member of this family, calycon (Caly), which directly interacts with μ subunits of AP-1, AP-2, and AP-3 (Muthusamy *et al.*, 2012). Caly binds the ubiquitous and neural-specific μ 3A and μ 3B subunit isoforms. Like AP-3, Caly is abundant in hippocampus (Zelenin *et al.*, 2002; Oakman and Meador-Woodruff, 2004). Studies in gene-targeted mice indicate that Caly regulates membrane attachment of AP-3 and sorting of AP-3 cargoes in axons (Muthusamy *et al.*, 2012). Since Caly directly interacts with the intermediate chain of cytoplasmic dynein (DIC) (Shi *et al.*, 2017), we investigated the hypothesis that it regulates the movement of AP-3 generated organelles in axons. Here we report that Caly increases bidirectional motility and raw numbers of these organelles and begin to define the molecular mechanism involved.

RESULTS

Caly regulates anterograde and retrograde motility of lysosomes in axons

Our previous studies showed that Caly directly interacts with DIC (Shi *et al.*, 2017). In the present study, we explored whether Caly could also play a role in axonal transport and specifically sought to test the hypothesis that Caly regulates dynein. We investigated this question in adult rat dorsal root ganglion (DRG) neurons transfected with a GFP-tagged Caly shRNAi (Caly RNAi) plasmid. Organelle transport is readily studied in DRG neurons due to the polarized orientation of microtubules in the axon-like processes extended by these cells in which movement toward the soma depends on the minus-end-directed motor dynein. We used the low pH-sensitive dye LysoTracker to label acidic organelles, including lysosomes, because retrograde movement of these organelles in axons is dynein dependent. In addition, we focused on LysoTracker motility because Caly did not colocalize with the MitoTracker mitochondrial stain (Supplemental Figure 1). We predicted that if endogenous Caly stimulates dynein, then Caly RNAi should reduce retrograde movement of LysoTracker-labeled vesicles. Knockdown (KD) of endogenous Caly in axons was confirmed by staining with an antibody to

Caly (Shi *et al.*, 2017), although the protein was still present in cell bodies after 48 h when time-lapse recordings were made (Figure 1A). LysoTracker-labeled organelles were less numerous in CalyKD axons (Figure 1, B and C). While the average speed and run length of motile events were similar in CalyKD and control axons (Figure 1, D and E), the percentage of static LysoTracker-labeled organelles was greater in Caly RNAi expressing axons (Figure 1F). Differences in the percentage of anterograde and retrograde events moving over 40 μ m further indicated that Caly KD altered LysoTracker organelle transport in axons. In CalyKD axons, long-distance anterograde motile events were more common, whereas long-distance retrograde ones were less common (Figure 1G). These data indicate that reducing the amount of endogenous Caly protein in axons lowered the capacity of LysoTracker-labeled organelles to undergo sustained retrograde transport. Alternatively, organelles might be less able to switch from anterograde to retrograde when Caly levels are reduced. Altogether, the data are consistent with the hypothesis that Caly modulates microtubule-dependent organelle motility. They also raise possibility that Caly levels regulate organelle number.

Interdependence of microtubule motor and adaptor protein complex binding to Caly

To better understand the regulation of LysoTracker-labeled organelle motility, we sought to test whether binding of dynein to Caly could depend on its interaction with heterotetrameric adaptor proteins. The location of the dynein binding site was refined by pull-down studies with truncations of the Caly C-terminus fused to glutathione-S-transferase (GST) and a preparation of highly purified dynein protein complex isolated from brain (Figure 2A). These studies indicated that the minimal segment capable of binding dynein spans residues 104–124, while fusion proteins including additional residues (GST-Caly104–140 and GST-Caly-104–217) were more effective in pulling down dynein (Figure 2B). In contrast, fusion proteins lacking residues 104–113 (GST-Caly-114–217 and GST-Caly-114–155) failed to bind dynein (Figure 2C). Altogether, these results indicate that residues 104–113 are critical for interaction of Caly with dynein.

We assessed the potential interdependence of dynein and adaptor protein complex binding by probing blots of GST-Caly pull downs of mouse brain lysates with antibodies to dynein, dynein adaptors, and adaptor protein complex subunits (Figure 3A). We also probed the blots with antibodies to the well-studied axonal kinesin KIF5a since Caly RNAi altered anterograde in addition to retrograde movement. GST-Caly-Wildtype (WT) pulled down dynein intermediate chain (DIC); however, a Caly truncation (GST-Caly-114–217) lacking residues 104–113 that are critical for dynein binding (Figure 2) was unable to pull down DIC. Similar findings were obtained with the dynein regulators Lis1 and the p150 subunit of dynactin (p150 Glued) as both were robustly pulled down by GST-Caly-104–217 but not by GST-Caly-114–217. Interestingly, the anterograde motor KIF5a was also present in the pull downs with the Caly C-terminus containing the critical dynein binding residues. KIF5A could therefore bind to Caly directly or indirectly via Lis1 or DIC (Yamada *et al.*, 2008; Twelvetrees *et al.*, 2016).

Caly binds AP-1, AP-2, and AP-3 μ subunits via a Yxx ϕ motif spanning residues 133–136, and mutation of this motif to 133-ATEA-136 abrogates binding (Muthusamy *et al.*, 2012). As expected, the ATEA mutation largely inhibited (e.g., AP-1 and AP-2) or abolished (e.g., AP-3) pull down of adaptor protein complex subunits compared levels recovered with wild-type GST-Caly. Surprisingly, the ATEA mutant also failed to pull down DIC, KIF5A, or Lis1. Nevertheless, long exposure of blots revealed a faint band

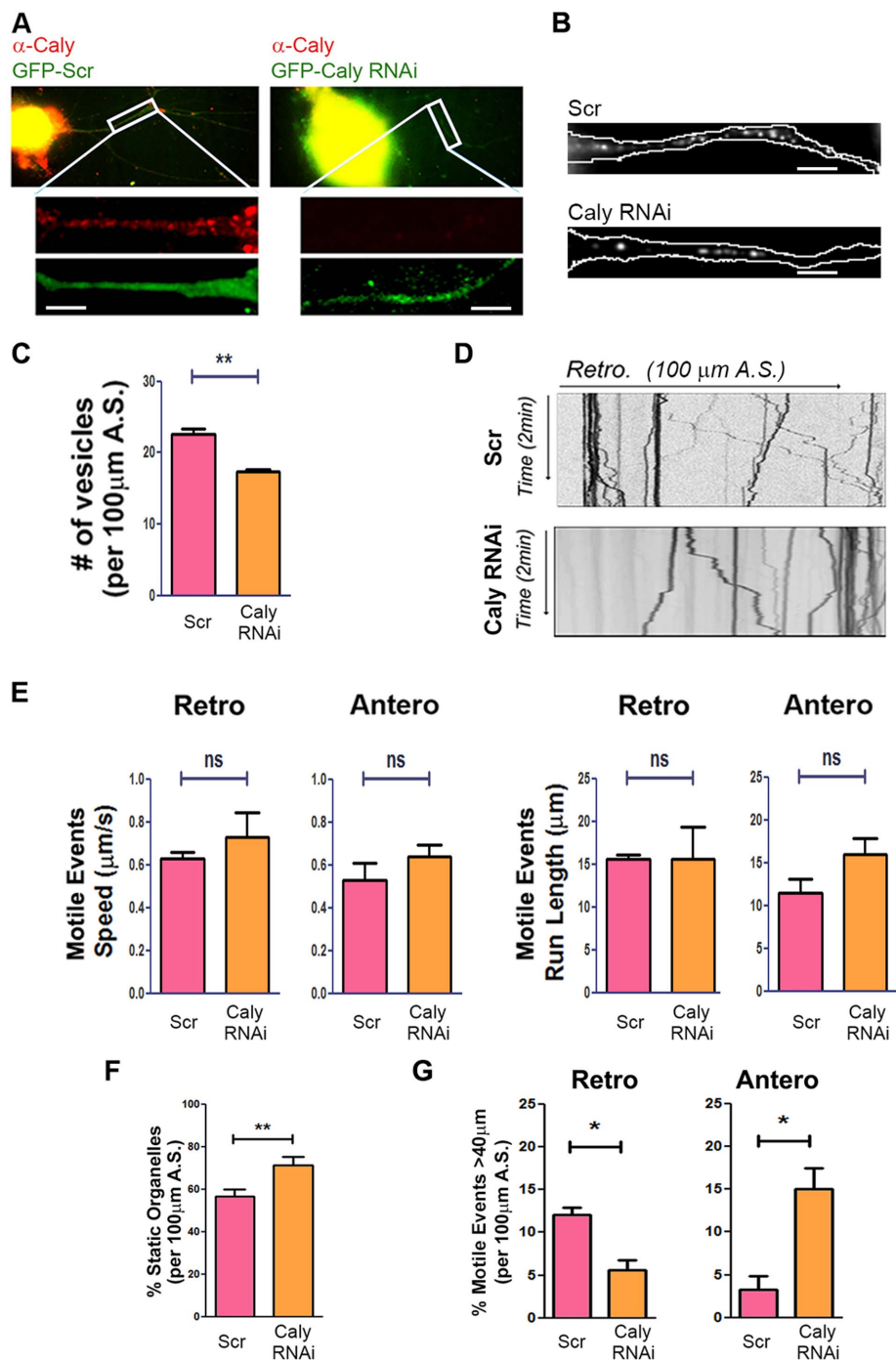


FIGURE 1: CalyKD reduces LysoTracker-labeled organelle motility. (A) Reduced Caly antibody staining (red) of DRG axons transfected with GFP-tagged Caly siRNA (Caly RNAi) compared with GFP-tagged scrambled RNAi (Scr)-transfected axons. (B) Representative micrographs of LysoTracker stained DRG axons transfected with GFP-Caly RNAi or Scr. Axons are outlined in white. (C) Number of LysoTracker positive vesicles in 100- μ m axon segments of DRG neurons transfected with GFP-Caly RNAi or GFP-Scr RNAi. Fewer LysoTracker positive vesicles were detected in Caly RNAi-transfected axons. (D) Kymographs of LysoTracker-labeled organelles in axons transfected with Scr or Caly RNAi. (E) Average speeds and run lengths of both anterograde and retrograde motile events from Caly RNAi-transfected axons do not differ from control. (F) Caly RNAi increased the percentage of static organelles. (G) Long-distance (>40 μ m) retrograde trajectories were more common in Scr axons, whereas long-distance anterograde trajectories were more common in Caly RNAi axons. Data shown in bar graphs reflect results obtained in three independent experiments, including at least five axons per group in each experiment; * $p < 0.05$, ** $p < 0.01$; A.S., axon segment; bar = 20 μ m.

suggesting that the ATEA mutant was able to precipitate low levels of the p150 Glued subunit of dynactin, indicating that additional epitopes could mediate interaction with dynactin (Figure 3A). However, deletion of residues critical for dynein binding resulted in greater recovery of AP-3 complex, suggesting that adaptor protein and motor protein binding to Caly are interdependent and that there could even be competition between dynein and AP3 for binding. Altogether, these results suggest that Caly is part of a multifunctional protein complex that is involved in vesicle sorting as well as microtubule-dependent transport.

Dependence of LE/LRO associated dynein levels on Caly and adaptor protein binding

Because adaptor proteins in brain extract had such a profound impact on Caly interactions with motor proteins, we next sought to test the hypothesis that defective binding of adaptor proteins would impair the ability of Caly to stimulate microtubule dependent motility. On the basis of the ability of Caly KD in DRG axons to reduce LysoTracker-labeled organelle motility, we predicted that overexpression of Caly (Caly-WT) would increase retrograde movement of these organelles, whereas expression of the adaptor protein binding mutant (Caly-ATEA) would fail to stimulate motility. To address this, we first confirmed that adaptor proteins are endogenously expressed in DRG axons by immunohistochemistry (Figure 3B). Axons were identified as structures stained by the neuron specific class III β tubulin beta (Tuj-1). AP-1 and AP-3 were present in cell bodies as well as throughout Tuj-1-labeled axons of DRG neurons, whereas AP-2 was detected only in cell bodies.

We next investigated whether adaptor protein binding to Caly impacted organelle motility in axons. We focused on AP-1 and AP-3 associated organelles since AP-2 levels in axons were negligible (Figure 3B). Both AP-1 and AP-3 sort cargoes from early/sorting endosomes (EE/SEs), whereas AP-3 plays a role in the biogenesis of both LE/LROs and synaptic vesicles (SVs) (Danglot and Galli, 2007; Newell-Litwa et al., 2007). We first examined whether the adaptor protein binding site mutation impacted the organelle distribution of Caly by expressing WT Caly or the ATEA mutant tagged with mCherry (mCh-Caly-WT and mCh-Caly-ATEA) in axons. We confirmed mCh-Caly-WT and mCh-Caly-ATEA localization in EE/SEs, LE/LROs, and SVs labeled by GFP-Rab5 or by antibodies to the lysosomal protein LAMP1 or PI4KII α .

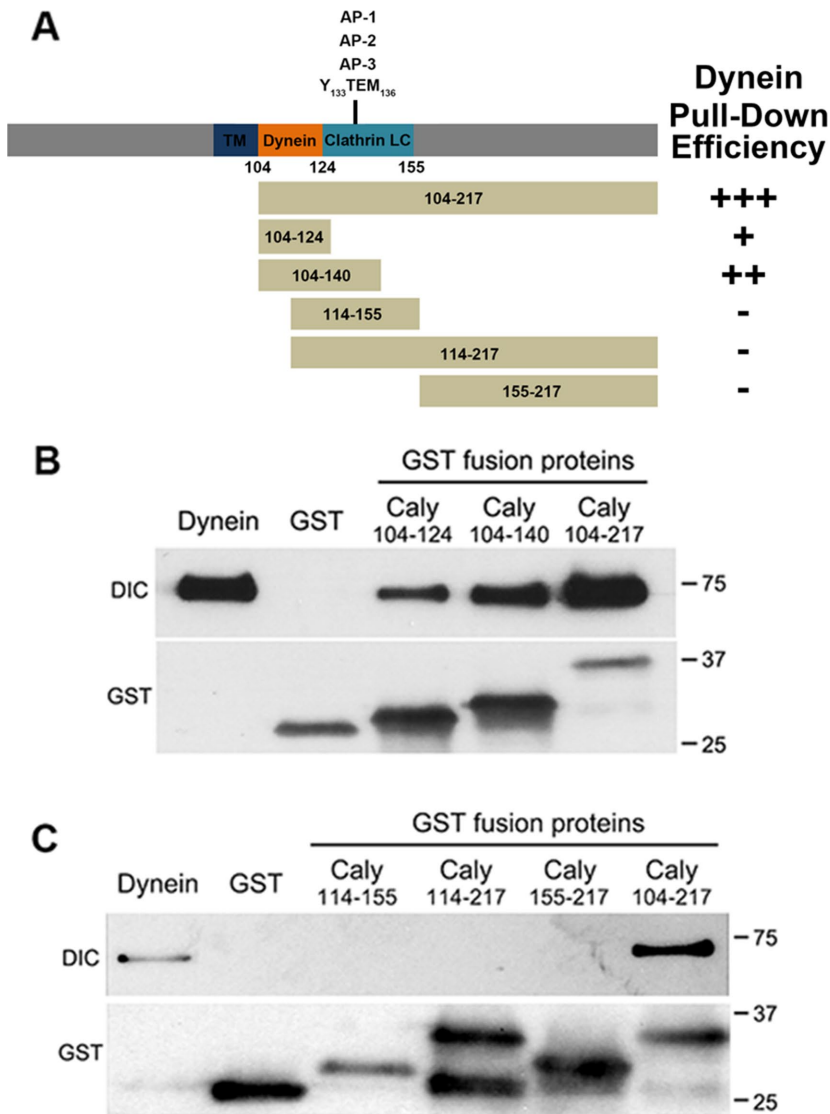


FIGURE 2: Mapping of dynein binding domain in Caly. (A) Stick figure diagrams the domain organization of the Caly protein, and the segments of Caly fused to GST for pull-down studies. Plus/minus (+/-) signs indicate effectiveness of respective GST fusion protein in pulling down purified bovine brain dynein. (B, C) Immunoblots of pull-down experiments probed with antibodies to DIC and GST. The "Dynein" lane in each blot was loaded with 5 μ g of purified dynein. The remaining lanes were loaded with resin-bound material eluted following incubation of GST Caly fusion proteins with the purified dynein complex (100 μ g protein). (B) The GST fusion containing juxtamembrane residues 104–124 was the shortest Caly fusion able to pull down dynein. (C) GST-Caly 114–155 was ineffective at pulling down dynein, suggesting that the relevant binding domain lies between residues 104 and 114.

PI4KII α phosphorylates phosphatidylinositol lipids on the 4' position; it associates with Golgi, SV, and endosomal membranes via palmitoylation; it is also both a cargo and a regulator of AP-3 directed sorting to lysosomes (Craigie *et al.*, 2008; Robinson *et al.*, 2014). Comparisons of the distribution of mCh-Caly-WT and mCh-Caly-ATEA in GFP-Rab5, LAMP1, and PI4KII α -positive organelles revealed significant differences (Figure 4, A–C). WT Caly localized to more than twice as many LAMP1 and PI4KII α positive organelles ($p < 0.001$ for both types of organelles) (Figure 4, A and B) than Caly-ATEA, whereas the opposite was true for GFP-Rab5-labeled organelles ($p < 0.001$) (Figure 4C). Taken together, these data suggest that the ability to bind adaptor proteins strongly influences the endosomal distribution of Caly. We also examined the overlap

of AP-3 with Caly WT or Caly ATEA in DIC-associated vesicles. This analysis showed significantly higher colocalization of AP-3 and Caly WT with DIC (Figure 4D) suggesting that adaptor protein binding also influences the association of dynein with Caly positive vesicles.

Since Caly-ATEA failed to pull down dynein and also exhibited lower colocalization with LE/LRO and SV markers, it may be less capable of recruiting dynein to LAMP1 and PI4KII α -labeled vesicles. If so, then levels of dynein associated with these vesicles in Caly-ATEA-transfected axons would be reduced compared with WT Caly axons. Immunofluorescence studies revealed that mCh-Caly increased the proportion of LAMP1 and PI4KII α -vesicles labeled by DIC antibody compared with mCherry control vector-transfected axons (Figure 5). This was not the case for mCh-ATEA. Moreover, reducing Caly levels by Caly RNAi lowered the percentage of DIC-labeled LAMP1 or PI4KII α vesicles by 50% (Figure 5). Taken together, the DIC organelle colocalization data indicated that Caly in conjunction with adaptor protein complexes could be involved in recruiting dynein to LE/LROs and SVs.

Dependence of LE/LRO number on Caly and adaptor protein binding

We next examined whether the adaptor protein binding site mutation impacted raw numbers of LAMP1 and PI4KII α vesicles. Counting of antibody-stained organelles revealed significantly fewer LAMP1 and PI4KII α -positive vesicles in mCh-Caly-ATEA-transfected axons compared with either mCh or mCh-Caly-WT-transfected axons (Figure 6A). Relative to scrambled RNA interference (RNAi)-transfected axons, KD of Caly with Caly RNAi also correlated with a significant reduction of LAMP1 and PI4KII α -positive vesicles (Figure 6, B and C). These data suggest that AP-3-dependent sorting of Caly impacts numbers of LE/LROs. The greater association of WT Caly with these vesicles could enhance

recruitment of dynein to them. Although Caly is predominantly expressed in neurons, we sought to confirm this finding by asking whether Caly influenced LE/LRO numbers in heterologous cells. Consistent with this notion, more Rab7 antibody-stained LE/LROs were detected in Cos-7 cells transfected with mCh-Caly-WT, while fewer Rab7 positive organelles were found in cells expressing mCh-Caly-ATEA (Supplemental Figure 2). In contrast, fewer EEA1 antibody stained EEs were detected in Caly WT compared with mCh control-transfected cells, whereas nearly twice as many EEs were detected in Caly-ATEA-transfected cells (Supplemental Figure 2). These results support the idea that sorting of Caly to LE/LROs impacts organelle numbers and that defects in adaptor protein binding prevent this.

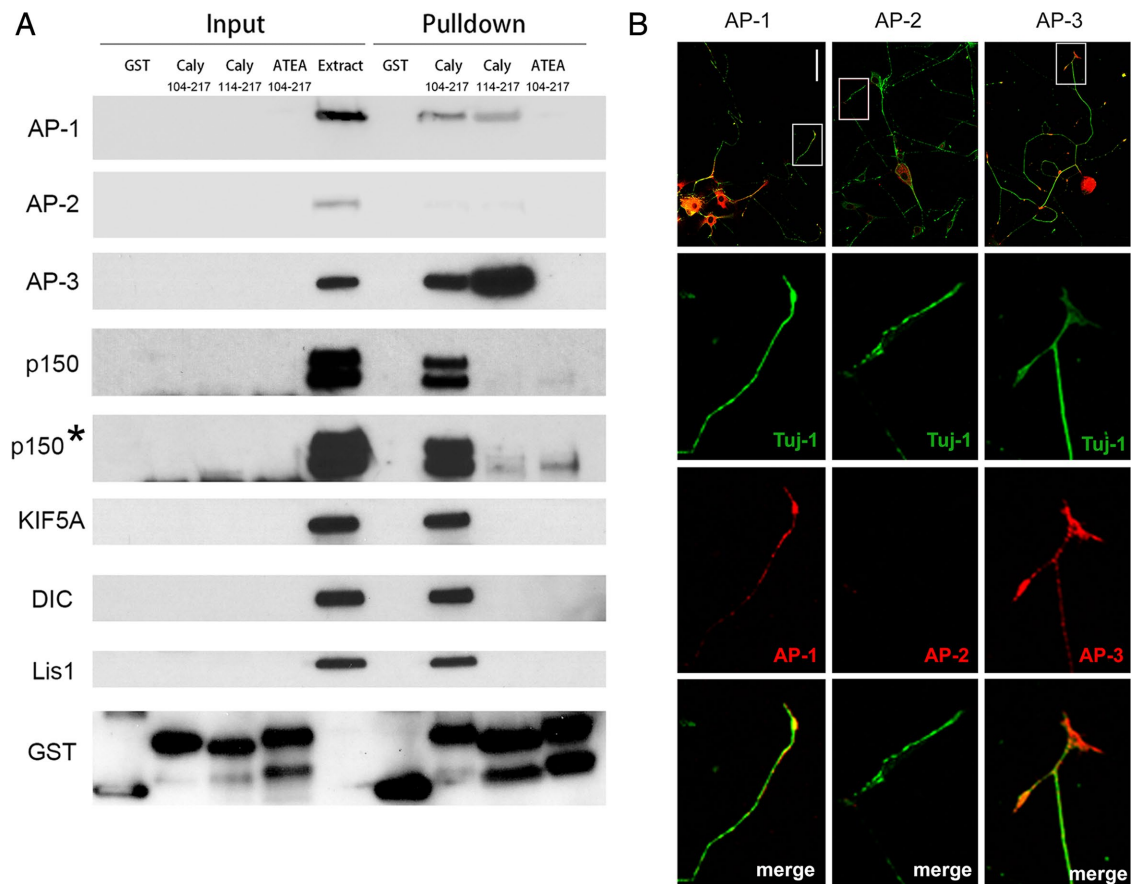


FIGURE 3: Association of Caly with microtubule motor and adaptor protein complexes. (A) Immunoblots of pull-down studies using brain homogenates and Caly GST fusion proteins indicated. Input lanes were loaded with 2% of brain homogenate (extract) or indicated resin bound GST protein used in the incubation. Pull-down lanes were loaded with 40% of the resin bound material eluted following incubation of GST Caly fusion proteins with homogenates of mouse brain (2 mg). Blots were probed with antibodies specific for the proteins shown and exposed for 15 s or less. Asterisk indicates blot from 15-min exposure of the anti-p150 signal. (B) Confocal micrographs of DRG axons stained with antibodies to neuron specific class III β tubulin beta (Tuj-1) (green) and the β , α , and δ subunits of AP-1, AP-2 and AP-3, respectively. Bar = 100 μ m.

Dependence of LE/LRO motility in axons on Caly and adaptor protein binding

On the basis of pull-down studies, as well as DIC organelle colocalization, we hypothesized that overexpression of WT Caly, but not the adaptor protein binding mutant ATEA, would increase the motility LE/LROs and SVs carrying AP-3 cargoes. We measured the motility of EE/SEs, LE/LROs, and SVs in DRG axons labeled by GFP-Rab5, LysoTracker, and EGFP-PI4KII α . Expression of mCh-Caly-WT increased the speed and run length of both retrograde and anterograde moving LysoTracker-labeled organelles (Figure 7, A and B). In contrast, expression of mCh-Caly-ATEA did not alter the motility of LysoTracker organelles, suggesting that adaptor protein binding plays an important role in either recruiting microtubule motors or stimulating transport (Figure 7, A and B). Expression of mCh-Caly-WT, but not mCh-Caly-ATEA, increased the percentage of organelles that moved retrogradely compared those that remained static or switched directions (Figure 7C). WT Caly expression also correlated with an increase in distance traveled by LysoTracker organelles during motile events (Figure 7D). Indeed, a third of the retrograde motile events in the mCh-Caly-WT axons exceeded 40 μ m. Surprisingly, 15% of motile events in the anterograde direction also exceeded 40 μ m in these axons. In contrast, motile events over 40 μ m either in the retrograde or anterograde direction were rarely observed in mCh or mCh-Caly-ATEA axons.

Like LysoTracker-labeled organelles, EGFP-PI4KII α -labeled organelles moved rapidly in axons, exhibiting a bias toward retrograde movement (Figure 8A). However, overall levels of PI4KII α -positive organelle motility were lower and more variable than observed for LysoTracker organelles. Nevertheless, analysis of speed and run lengths of individual motile events revealed that WT Caly expression increased both parameters and also stimulated movement of PI4KII α -positive organelles in both directions (Figure 8B). In contrast, neither average speed nor average run length in the Caly-ATEA axons differed from mCh control axons (Figure 8B). The percentage of retrograde moving PI4KII α -positive organelles relative to static organelles were increased in Caly-WT but not Caly-ATEA axons (Figure 8C), whereas long-distance motile events were unaffected by expression of either Caly variant (Figure 8D). Taken together, the results of kymograph analyses of LysoTracker-labeled (Figure 7) and PI4KII α -positive (Figure 8) organelles suggest that in conjunction with adaptor proteins, Caly stimulates microtubule-based transport of AP-3 generated organelles in axons.

AP-1 and AP-3 bind tubules on EE/SEs and sort cargoes into vesicle carriers. We therefore also evaluated whether either WT or the adaptor protein binding site mutant of Caly altered the motility of EE/SEs labeled with GFP-Rab5. While comparable with previous reports of EE/SE speed and run lengths, GFP-Rab5-positive organelle motility in axons was much lower than that of either

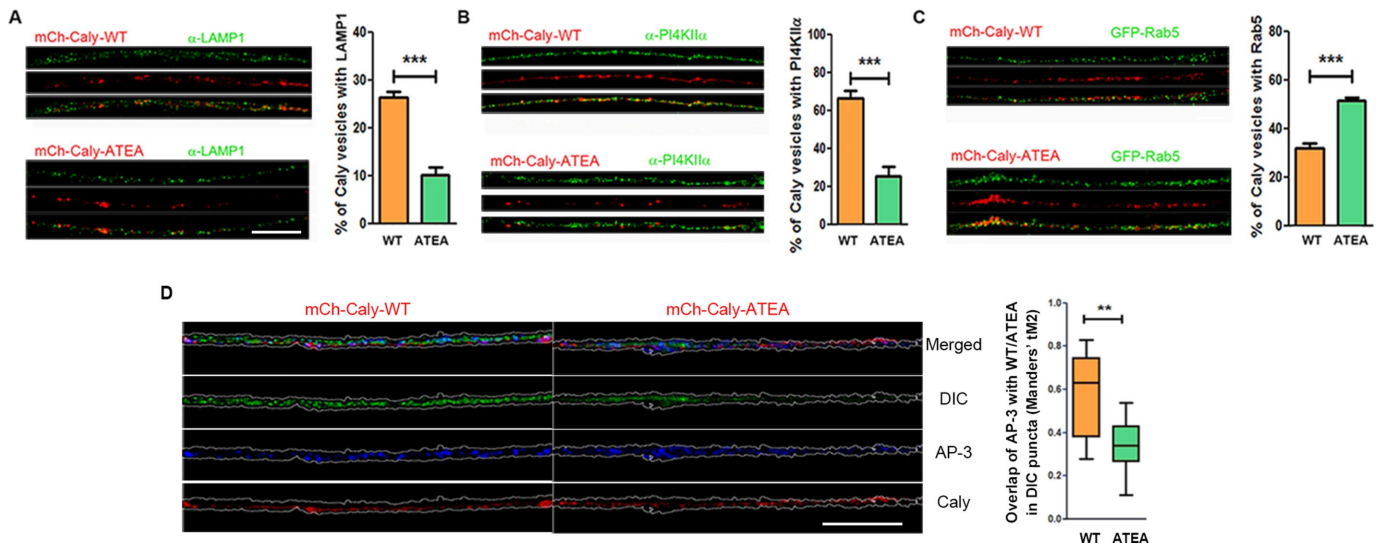


FIGURE 4: Caly sorting requires interaction with adaptor protein complexes. (A–C) Differential localization of Caly-WT and Caly-ATEA in EE/SEs and LE/LROs. Confocal micrographs of DRG axons transfected with mCh-Caly-WT or mCh-Caly-ATEA (red) and stained with LAMP1 (A) or PI4KII α (B) antibodies or cotransfected with GFP-Rab5 (C) (green). Bar graphs show the mean and SEM of overlapping red and green puncta in 100- μ m axon segments of each group. (D) Confocal micrographs of DRG axons transfected with mCh-Caly-WT or mCh-Caly-ATEA (red) and stained with DIC (green) and AP-3 (blue). Manders coefficient of overlap was determined for colocalization of Caly-WT or Caly-ATEA with AP-3 in DIC positive puncta. Caly-WT exhibited greater colocalization with AP-3/DIC positive puncta than Caly-ATEA. Box-and-whisker plots show the Manders's tM2 of overlapping red and blue puncta in 100- μ m axon segments of each group. Data plotted in histograms or in box-and-whisker plots correspond to results obtained in three independent experiments from at least five axons per experiment for each group; ** $p < 0.01$, *** $p < 0.001$; bar = 20 μ m.

LysoTracker or PI4KII α -positive organelles (Craigie et al., 2008; Robinson et al., 2014). Surprisingly, despite exhibiting no effect on the LysoTracker and PI4KII α -positive organelle motility, Caly-ATEA appeared to stimulate EE/SE motility. The speed of both anterograde and retrograde moving GFP-Rab5-labeled organelles was increased in Caly-ATEA expressing axons compared with control or WT Caly-transfected axons (Figure 9, A and B). No differences in levels of GFP-Rab5-labeled organelle motility were detected in mCh-Caly-WT compared with mCh-transfected axons. In contrast, there were fewer static and more retrograde moving organelles in Caly-ATEA axons, but no alterations in long-distance motile events (Figure 9, C and D). These alterations in movement further indicate that the role of Caly in organelle motility is dependent on adaptor protein binding, while also indicating that vesicle context is a critical factor.

DISCUSSION

Substantial progress has been made in defining the roles of dynein and kinesin in axonal transport. However, much less is known about the molecules and mechanisms involved in coupling motor proteins with axonal organelles. Active transport of organelles in axons is critical for communication between the synapse and cell body (Hinckelmann et al., 2013; Maday et al., 2014). The LE/LRO system, in particular, is essential for supplying axonal constituents and synaptic cargoes as well as for removing damaged proteins and lipids. The present study identifies a novel mechanism regulating the transport and number of LE/LROs in axons based on the coupling of microtubule motor and vesicle coat protein complexes. Multiple lines of evidence suggest that the transmembrane protein Caly could coordinate the coupling of motor and adaptor protein complexes in this mechanism as discussed below.

Our results revealed a positive correlation between LysoTracker and PI4KII α positive organelle movement and Caly levels, consistent

with the idea that Caly regulates axonal transport. Based on pull-down and motility studies, our findings indicate that Caly could promote dynein/dynactin attachment. Motor adaptors like BicaudalD2, Hook1, and Hook3 stabilize the dynein/dynactin complex resulting in increased motor processivity and longer run lengths (Carter et al., 2016; Olenick et al., 2016; Schroeder and Vale, 2016). Alterations in sustained attachment or motor processivity would be expected to impact long-distance motile events and could potentially contribute to the divergent effects of Caly-WT and CalyRNAi on LysoTracker motile events over 40 μ m. Nevertheless, our data cannot distinguish whether Caly might selectively regulate either the initial recruitment of motors or their sustained attachment. Whatever the underlying mechanism, the effects of Caly on axonal transport appear to be specific for LE/LROs since expression of Caly-WT failed to stimulate the motility of EE/SEs. Organelle specific functions are common among motor adaptor and scaffolding proteins; Bicaudal D2, for example, stimulates dynein when the motor is associated with Rab6 positive organelles (Schlager et al., 2014). However, greater EE/SE motility was detected in Caly-ATEA axons. While the mechanism underlying this response remains to be worked out, the ability of Caly-ATEA to bind dynactin and/or its accumulation in EE/SEs could be contributing factors. Alternatively, since proteomic data suggest that Caly can form homodimers (C.B., unpublished data), the increased motility of EE/SEs in Caly-ATEA axons could involve association of the adaptor protein binding defective mutant with endogenous Caly.

Bidirectional movement is typical of axonal LE/LROs and is driven by dynein and kinesin (Maday et al., 2014). Our findings indicate that expression of Caly-WT in axons stimulates both anterograde and retrograde movement of these organelles, which differentiates it from the biogenesis of lysosome-related organelles

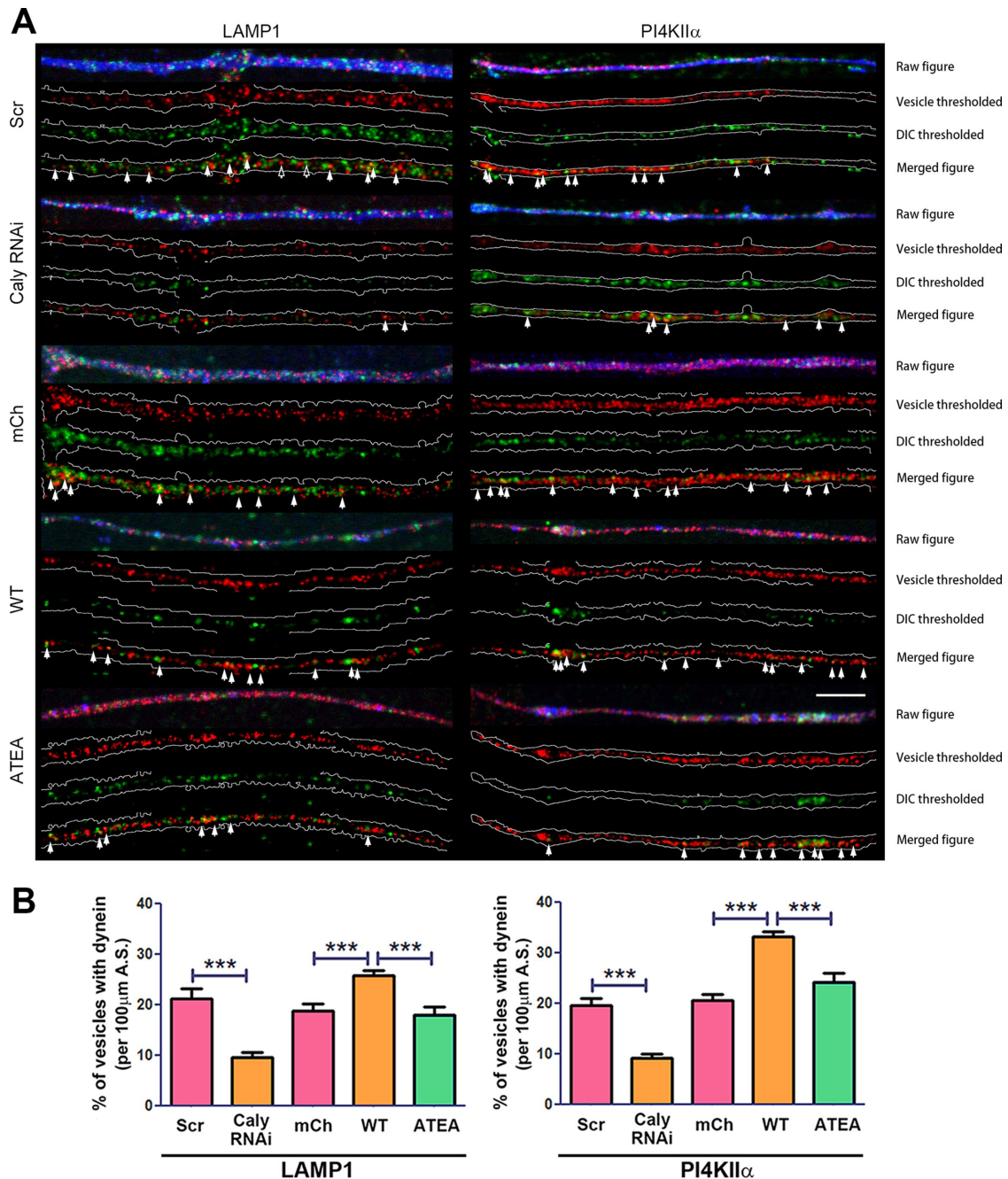


FIGURE 5: Caly stimulated dynein recruitment requires interaction with adaptor protein complexes. (A) Dynein labeling of LE/LROs in DRG axons transfected with GFP-Caly RNAi, GFP-Scr RNAi, mCherry vector, mCh-Caly-WT, or mCh-Caly-ATEA and stained with LAMP1 and PI4KII α antibodies. Axons are outlined in white; filled arrows point to overlapping puncta, whereas hollow arrows show the examples of nonoverlapping puncta. (B) Greater dynein colocalization with LAMP1- or PI4KII α -positive organelles is detected in Caly-WT-transfected axons, whereas less is observed in Caly RNAi-transfected axons. Data plotted in bar graphs correspond to results obtained in three independent experiments from at least five axons per experiment for each group; *** $p < 0.001$; bar = 10 μ m.

complex 1 (BLOC-1) subunit, snapin. Like Caly, snapin stimulates LE/LRO motility but only in the retrograde direction (Cai *et al.*, 2010). Pull-down studies indicated that Caly associates with both anterograde and retrograde motor proteins in brain, consistent with its bidirectional effects on motility. Taken together, these findings suggest that Caly could be a scaffolding protein for both kinesin and dynein motor complexes, as has been shown for a number of other motor scaffolding proteins including Milton/TRAK, Huntingtin, and

JIP1-4 (Fu and Holzbaaur, 2014). They also raise the possibility that Caly could coordinately regulate the recruitment of both anterograde and retrograde motors. Since kinesin motors generate four to eight times more force than cytoplasmic dynein, it will be interesting to learn how the roughly equivalent effect of Caly overexpression on anterograde and retrograde movement is achieved (Müller *et al.*, 2008). Results showing that Lis1 and the p150 glued subunit of dynactin are also associated with Caly could be relevant to this

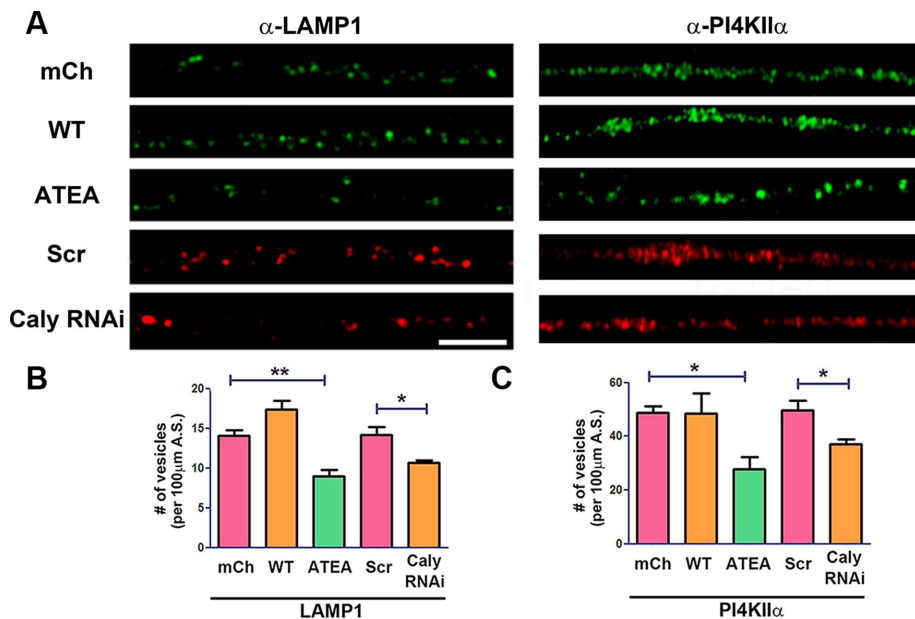


FIGURE 6: LE/LRO biogenesis requires interaction with adaptor protein complexes. (A) Labeling of LE/LROs in DRG axons transfected with GFP-Caly RNAi, GFP-Scr RNAi, mCherry vector, mCh-Caly-WT, or mCh-Caly-ATEA by LAMP1 or PI4KII α antibodies. Number of LAMP1 (B) or PI4KII α (C) antibody-labeled vesicles in 100- μ m axon segments of DRG neurons transfected with GFP-Caly RNAi, GFP-Scr RNAi, mCherry vector, mCh-Caly-WT, or mCh-Caly-ATEA. Fewer LAMP1 and PI4KII α antibody-labeled vesicles were detected in Caly RNAi and Caly-ATEA-transfected axons. Data plotted in bar graphs correspond to results obtained in three independent experiments from at least five axons per experiment for each group; * $p < 0.05$, ** $p < 0.01$; bar = 10 μ m.

question since both proteins strongly activate dynein (King and Schroer, 2000; Smith *et al.*, 2000; Pandey and Smith, 2011; Bely *et al.*, 2016).

Increased LE/LRO transport in axons correlated with the ability of Caly to bind to the heterotetrameric adaptor protein complexes AP-1, AP-2, and AP-3. Likewise, interaction with adaptor protein complexes regulated the distribution of Caly in axonal organelles. AP-1 and AP-3 are expressed throughout DRG axons; however, while we cannot absolutely exclude a role for AP-1, various aspects of the results strongly implicate AP-3 in the mechanism. 1) Organelle specificity: AP-3 sorts axonal cargoes to LE/LROs and SVs, whereas AP-1 sorts cargoes to other types of endosomes and secretory granules (Bonifacio, 2014). In addition, previous studies in nonneuronal cells raised the possibility that AP-3 could play a role in the association of LE/LROs with microtubules. For example, lysosome movement is abolished in cytotoxic T lymphocytes from individuals with Hermansky-Pudlak syndrome type 2 (HSP2), which is caused by a deficiency in the AP-3 complex (Clark *et al.*, 2003). Also, in fibroblasts, KD of AP-3 disrupts alignment of lysosomes along microtubules (Ivan *et al.*, 2012). 2) Interdependence of motor protein and adaptor protein complex binding: pull-down studies revealed that dynein binding regulated interaction of Caly with AP-3 but not with AP-1 or AP-2. Likewise, motor protein binding to an adaptor protein binding-defective mutant of Caly was much weaker (e.g., p150 Glued), and in most cases, abolished (e.g., dynein, Lis1, KIF5A) compared with wild-type Caly. Together, these results indicate that AP-3 and microtubule motor protein binding to Caly could be linked, and perhaps even be competitive. 3) Alternatively, AP-3 could independently associate with microtubule motors. This notion is supported by a proteomic analysis of the AP-3 interactome in PC12 cells in which dynactin as well as several subunits of cytoplasmic dynein were copurified with

chemically cross-linked AP-3 (Salazar *et al.*, 2009). This possibility is also consistent with the different abilities of wild type and the adaptor protein binding-defective mutant of Caly to pull down motors from brain as observed in the present studies. As discussed in detail below, an involvement of AP-3 in motor recruitment as well as cargo sorting could also be relevant to understanding the organelle specific differences in motility observed in our studies.

Our data are also consistent with the possibility that the stimulatory effects of Caly on motility could pertain to distinct subpopulations of LE/LROs. For example, the increase in motility of LysoTracker-labeled organelles in Caly-WT axons was four times that of PI4KII α -positive organelles. Likewise, overall levels of PI4KII α -positive organelle motility were also lower and more variable compared with LysoTracker organelles. AP-3 sorts PI4KII α to SVs as well as LE/LROs, but the current data cannot distinguish whether Caly promotes PI4KII α positive SV and LE/LRO motility to an equal extent. In addition, PI4KII α -positive SVs and LE/LROs could be heterogeneous with respect to levels of associated motors. Consistent with this idea, one report suggests that the intrinsic motility of SVs is less than LE/LROs (Lorenzo *et al.*, 2014). Another possi-

bility is that PI4KII α itself plays a role in the organelle specific differences in motility because besides being an AP-3 cargo, it can recruit AP-3 to membranes (Craigie *et al.*, 2008; Salazar *et al.*, 2009). Nevertheless, the present findings provide several lines of evidence implicating AP-3 in axonal transport based on the ability of Caly to couple it with anterograde and retrograde motors. The functional relationship outlined here for AP-3 and Caly appears to be analogous to that described for AP-1 and Gadkin-1 which directly interacts with kinesin-1 and with AP-1. Similar to what we find for Caly and LE/LROs, Gadkin-1 stimulates movement of AP-1 generated organelles (Schmidt *et al.*, 2009; Maritzen and Haucke, 2010).

The current findings indicate that Caly sorting influences LE/LRO number and implicate its interaction with adaptor protein complexes in the underlying mechanism. Alternatively, Caly's effects on motility could be linked to its effects on biogenesis and might be specific for a select subpopulation of AP-3 generated organelles. In this regard, future studies could address whether Caly regulates the biogenesis and transport of other types of AP-3 generated organelles including SVs and DCVs (Grabner *et al.*, 2006; Asensio *et al.*, 2010; Sirkis *et al.*, 2013). The relationship of microtubule motors with vesicle coat proteins during organelle biogenesis is currently not well understood. However, recent studies indicate that biogenesis of REs and melanosomes involves the orchestrated association of the anterograde motor kinesin and AP-1 and BLOC-1 coat proteins with tubulovesicular structures on endosomes (Delevoye *et al.*, 2009, 2016). Since Caly increases the association of AP-3 with membranes (Muthusamy *et al.*, 2012), it is tempting to speculate that it could stimulate recruitment of AP-3 to budding LE/LROs and regulate AP-3-dependent vesicle formation. A mechanism based on increased recruitment could explain both the alterations in numbers of LE/LROs observed in CalyRNAi and Caly-ATEA-transfected axons, as

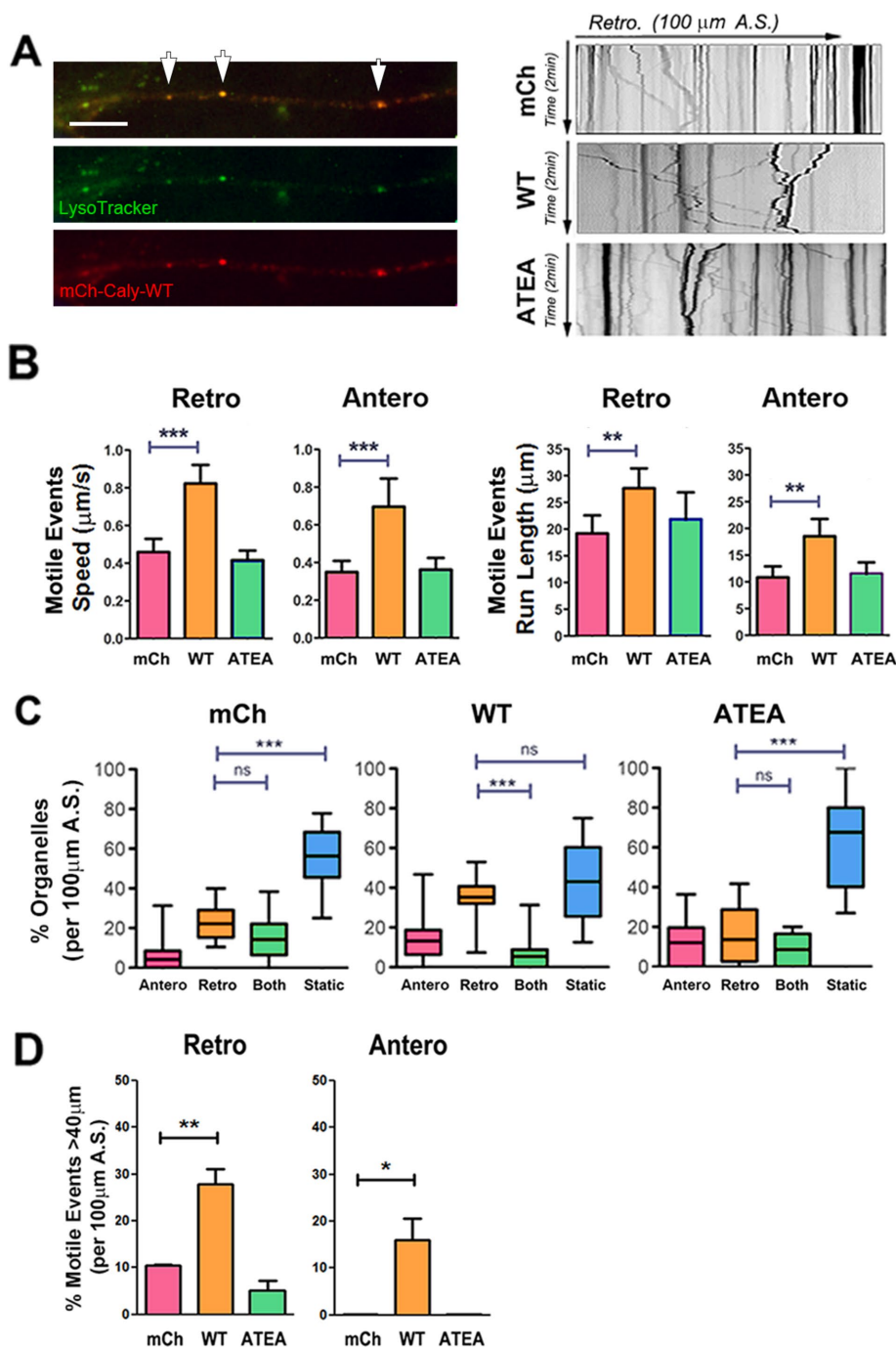


FIGURE 7: Caly-WT but not Caly-ATEA increases the motility of LysoTracker-labeled LE/LROs. (A) Left panels, colocalization of LysoTracker (green) and mCh-Caly-WT (red). Arrows point to overlapping puncta. Right panels, representative kymographs of LysoTracker-labeled organelles in axons transfected with mCherry (mCh), mCh-Caly-WT (Caly-WT), and mCh-Caly-ATEA (Caly-ATEA). (B) Average speeds and run lengths of anterograde as well as retrograde motile events are higher in Caly-WT axons, whereas values detected in Caly-ATEA axons do not differ from control. (C) Retrogradely moving LysoTracker-labeled organelles are more common in Caly-WT axons relative to static or bidirectional organelles. (D) Retrograde and anterograde motile events with long-distance (>40 μm) trajectories are more common in Caly-WT axons. Data shown in bar graphs (mean ± SEM) and box-and-whisker plots (mean ± 95% CI) reflect results obtained in three independent experiments, involving at least five axons per group in each experiment; * $p < 0.05$, ** $p < 0.01$, *** $p < 0.001$; A.S., axon segment, bar = 20 μm.

well as those detected in Caly-WT and Caly-ATEA-transfected Cos-7 cells. Proteomic data suggest that Caly can form homodimers (C.B., unpublished data), so Caly-ATEA might mask the function of endog-

enous Caly on biogenesis in axons. Clearly more research is needed to disentangle the exact roles of motor protein and adaptor protein complex interactions with Caly and to identify other factors in brain that regulate assembly and disassembly of this newly identified multifunctional protein complex.

The LE/LRO pathway is implicated in neurodegenerative disorders like Parkinson's, Huntington's, and Alzheimer's diseases that involve accumulation of misfolded proteins (Schreij *et al.*, 2016). The stimulatory effect of Caly overexpression on LE/LRO transport and vesicle number in axons is therefore particularly intriguing since induction of Caly expression was found to be neuroprotective in a primary culture model of glucose and oxygen deprivation (Dai *et al.*, 2010). Mutations in the Caly gene are associated with attention deficit hyperactivity disorder (ADHD), and expression of the gene is up-regulated in brains of patients with schizophrenia (Koh *et al.*, 2003; Bai *et al.*, 2004; Clinton *et al.*, 2005; Laurin *et al.*, 2005; Baracska *et al.*, 2006). Pinpointing the physiological significance of increased levels of Caly in schizophrenia, however, has remained elusive. In this respect, it will be interesting to explore whether the effects of Caly overexpression on LE/LRO number and axonal transport observed in the present studies could be part of a compensatory response to alterations induced by schizophrenia-associated mutations in the BLOC-1 subunit dysbindin, which also interacts with AP-3 (Talbot *et al.*, 2006; Jentsch *et al.*, 2009; Taneichi-Kuroda *et al.*, 2009; Ghiani *et al.*, 2010; Larimore *et al.*, 2011; Mullin *et al.*, 2011, 2015).

MATERIALS AND METHODS

Vectors and antibodies

Rat calcyon-specific shRNA in pGFP-V-RS (catalogue no. TG712969) and scrambled negative control shRNA in the same vector were purchased from Origene. mCherry, human Caly, or ATEA sequences were inserted in pCMV-tag3C vector. GST fused truncated Caly sequences were insert in pET-GST vector. GFP-PI4KIIα was a generous gift from Victor Faundez, Emory University. GFP-Rab5 (catalogue no. 31733) was purchased from Addgene. The sources and dilutions of primary antibodies used in immunofluorescence (IF) and Western blotting (WB) were as follows: DIC (WB: 1:1000, IF: 1:500, Santa Cruz, sc-13524, RRID:AB_668849) and Alexa Fluor 488 conjugated DIC (IF: 1:100, Santa Cruz, sc-13524 AF488, RRID:AB_668849); Lis1 (WB: 1:500, an in-house rabbit polyclonal antibody, Smith *et al.*, 2000); GST (WB: 1:2000, Santa Cruz, sc-459, RRID:AB_631586); rat Caly (IF: 1:500, Millipore, AB15040, RRID:AB_805266); KIF5A (WB:

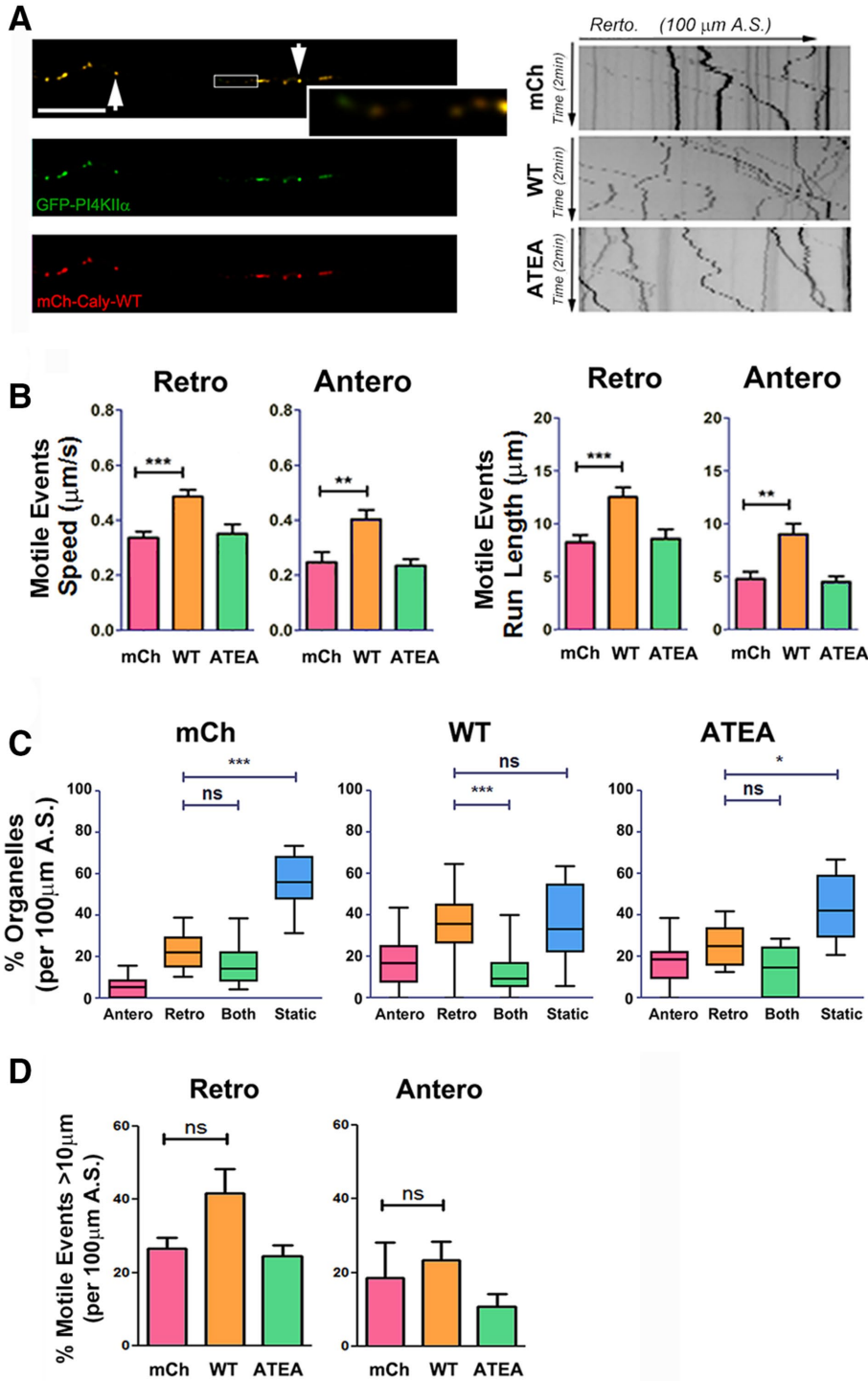


FIGURE 8: Caly-WT but not Caly-ATEA increases the motility of PI4KII α -labeled organelles. (A) Left panels, colocalization of GFP-PI4KII α (green) and mCh-Caly-WT (red). Arrows point to overlapping puncta, and enlarged box show some examples of nonoverlapping puncta. Right panels, representative kymographs of PI4KII α -labeled organelles in axons transfected with mCherry (mCh), mCh-Caly-WT (Caly-WT), and mCh-Caly-ATEA (Caly-ATEA). (B) Average speeds and run lengths of both anterograde and retrograde motile events are higher in Caly-WT axons, whereas values detected in Caly-ATEA axons do not differ from control. (C) Box-and-whisker plots show that retrogradely moving PI4KII α -labeled organelles are more common in Caly-WT axons relative to static and bidirectional organelles. (D) No difference in retrograde and anterograde motile events over >10 μ m were detected. Data shown in bar graphs (mean \pm SEM) and box-and-whisker plots (mean \pm 95% CI) reflect results obtained in three independent experiments, with at least five axons per group in each experiment; * p < 0.05, ** p < 0.01, *** p < 0.001; A.S., axon segment; bar = 20 μ m.

1:2000, abcam, ab5628, RRID:AB_2132218); p150 glued (WB: 1:1000, BD Biosciences, 610473, RRID:AB_397845); LAMP1 (IF: 1:1000, Millipore, AB2971, RRID:AB_10807184); PI4KII α (IF: 1:500, Thermo, PA5-15275, RRID:AB_2163898); AP-1 γ subunit (WB: 1:500, IF: 1:250, Sigma, A4200, RRID:AB_476720); AP-2 α subunit (WB: 1:500, IF: 1:250, Thermo, MA1-064, RRID:AB_2258307); AP-3 δ subunit (WB: 1:500, IF: 1:250, BD, 610385, RRID:AB_610385); Rab7 (WB: 1:1000, IF: 1:500, Cell Signaling, catalogue no. 9367, RRID:AB_1904103); Tuj-1 (IF: 1:1000, Neuromics, CH23005, RRID:AB_2210684); and EEA1 (IF: 1:1000, Synaptic Systems, 237 002, RRID:AB_10694097). The sources and dilutions of secondary antibodies used in IF and WB were as follows: horseradish peroxidase (HRP)-conjugated goat anti-rabbit and mouse (WB: 1:50,000; Millipore 12-348 and 12-349, RRIDs:AB_390191 and AB_390192); Alexa 647-conjugated goat anti-mouse and rabbit (IF: 1:1000, Jackson ImmunoResearch, 115-605-003 and 111-605-003, RRID:AB_2338902 and RRID:AB_2338072); Alexa 488-conjugated goat anti-mouse and rabbit (IF: 1:1000, Jackson ImmunoResearch, 115-545-003 and 111-545-003, RRID:AB_2338840 and RRID:AB_2338046). LysoTracker red and green (1:2000, Thermo, L7528 and L7526) were used to stain acid organelles in live cells.

GST pull down

Freshly dissected forebrains from wild-type (WT) c57bl/6 mice were homogenized in eight volumes of homogenization buffer (10 mM HEPES, pH 7.4, 320 mM sucrose) containing protease inhibitors (Thermo, catalogue no. 78430). Cytosolic fractions were prepared by ultracentrifugation at 100,000 \times g for 1 h and then precleared by incubating with glutathione resin (Amersham Biosciences), added at a 1:10 ratio, for 2 h at 4°C. Pull-down experiments were performed as described previously (Muthusamy *et al.* 2012). Briefly, equal amounts of glutathione-S-transferase (GST) and fusion proteins consisting of GST fused to truncations of human Caly (NCBI accession no. NP_056537) (Caly-1-94, Caly-104-217, Caly-114-217, Caly-104-155, etc.) or to a double point mutant human Caly (ATEA-104-217) were bound to glutathione resin and blocked with 5% bovine serum albumin in homogenization buffer. Precleared cytosolic fractions of brain (2 mg) or highly purified dynein complex from bovine brain (100 μ g) (generous gift of Steve King, University of Central Florida) were added to resins and nutated overnight at 4°C.

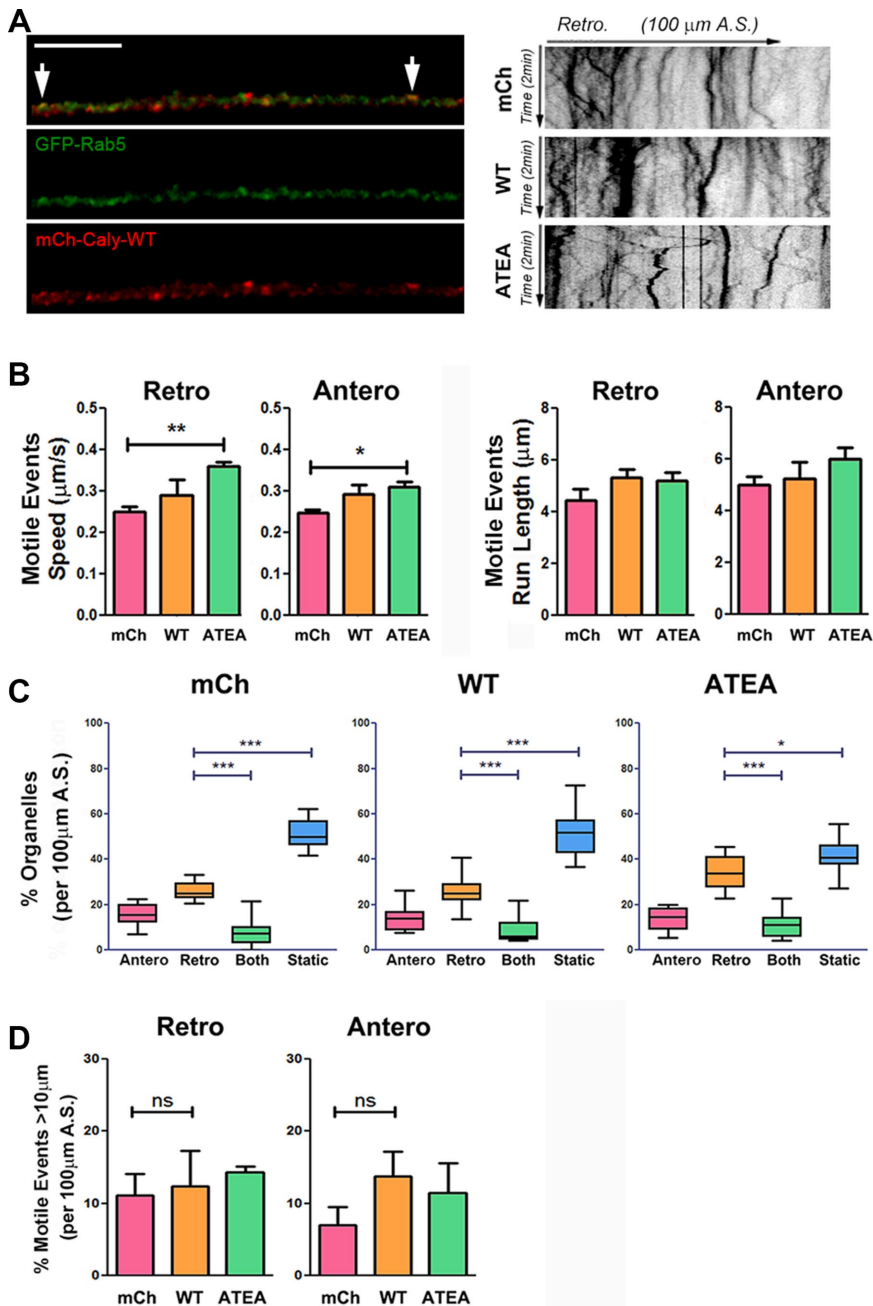


FIGURE 9: Caly-ATEA but not Caly-WT increases the motility of GFP-Rab5-labeled organelles. (A) Left panels, colocalization of GFP-Rab5 (green) and mCh-Caly-WT (red). Arrows indicate overlapping puncta. Right panels, representative kymographs of Rab5-labeled organelles in axons transfected with mCherry (mCh), mCh-Caly-WT (Caly-WT), and mCh-Caly-ATEA (Caly-ATEA). (B) Average speeds of anterograde and retrograde motile events are higher in Caly-ATEA axons, whereas values detected in Caly-WT axons do not differ from control. (C) Retrogradely moving Rab5-labeled organelles are more common in Caly-ATEA axons relative to static and bidirectional organelles. (D) No difference in retrograde and anterograde motile events $>10\mu\text{m}$ were detected. Data shown in bar graphs (mean \pm SEM) and box-and-whisker plots (mean, min, max \pm 95% CI) reflect results obtained in three independent experiments, with at least five axons per group in each experiment; * $p < 0.05$, ** $p < 0.01$, *** $p < 0.001$; A.S., axon segment; bar = $20\mu\text{m}$.

Proteins bound to glutathione resin were eluted after washing three times each with homogenization buffer and phosphate-buffered saline plus Triton (PBST), and resolved by SDS-PAGE, followed by transfer to polyvinylidene fluoride (PVDF) membranes. Blots were probed with primary antibodies followed by HRP-conjugated

secondary antibodies. Antibody binding was revealed by chemiluminescence (ECL Plus; GE Amersham).

Adult rat DRG cultures and transfection

All animal work was carried out under protocols approved by the University of South Carolina Animal Care and Use Committee. Primary cultures of sensory neurons were prepared from lumbar dorsal root ganglia (DRG) of adult rats as described (Smith and Skene, 1997). Neurons were plated onto German glass coverslips (Fisher) coated with $10\mu\text{g/ml}$ poly-D-lysine (Sigma) and $10\mu\text{g/ml}$ laminin (Millipore) and maintained at 37°C , 5% CO_2 in DMEM/F12 supplemented with 10% horse serum and 1X N1 additives. Neurons were transfected immediately after dissection using the SCN Basic Nucleofector kit for primary neurons (Amaxa Biosystems VSP1 catalogue no. 1003) (Pandey and Smith, 2011) and plated. Neurons were used for transport studies within 2–3 d of culture preparation.

Immunostaining of DRG neurons and Cos-7 cells

For Caly, AP-1, AP-2, AP-3, LAMP1, and PI4KII α staining, neurons were fixed in 4% paraformaldehyde 24–48 h after plating and then permeabilized with 0.1% Triton X-100 for 5 min at room temperature. For DIC costaining, neurons were fixed in 4% paraformaldehyde for 3 min and then in 100% ice-cold methanol for 2 min at -20°C . Transfected Cos-7 cells were fixed in 4% paraformaldehyde and stained with EEA1 or Rab7 antibodies. Nuclei were visualized with Hoechst, and coverslips were mounted on glass slides using ProLong Gold Antifade reagent (Invitrogen). Neurons were viewed with an Axiovert 200 (Carl Zeiss) equipped with Plan-Neo 100 \times /1.30 and Plan-Apo 63 \times /1.40 objectives, and images were acquired using a charge-coupled camera (AxioCam HRm; Carl Zeiss) linked to Axio-Vision software (version 4.7, Carl Zeiss). Confocal images of the Cos-7 cells were obtained with Zeiss 780 Inverted Confocal equipped with 63 \times Alpha Plan-Apo(oil)-NA 1.46 objective.

Fluorescence time-lapse microscopy in DRG axons

Coverslips were transferred into fresh medium containing 25 mM HEPES, pH 7.4, and 10 mM Oxyrase (Oxyrase). Time-lapse microscopy was performed using a Leica confocal microscope (SP8) with a 63 \times objective in a climate-controlled live-cell imaging enclosure. The zoom setting was set to sample the x/y plane at the Nyquist rate (512×64 pixels, zoom $\times 1.0 = 488\text{ nm/pixel}$). Axon segments that were clearly linked

to a specific neuronal cell body were selected for analysis. Digital images were acquired every 0.3 s for 2 min (400 frames).

Motility analyses

Kymographs were generated from time-lapse movies using the ImageJ software (version 1.43u, National Institutes of Health) and the KymoToolBox ImageJ plug-in (generous gift of Frédéric Saudou, Grenoble Institute of Neuroscience, University of Joseph Fourier, France) to differentiate motile and static organelles and to analyze motility. By convention the direction toward the cell body was always to the right, so lines that sloped toward the right at any point during the recording interval with a net displacement of $>5\ \mu\text{m}$ were categorized as retrograde organelles. Lines that sloped toward the left $>5\ \mu\text{m}$ at any time during the recording interval were considered anterograde organelles. Lines that switched directions one or more times were categorized as bidirectional, and lines that showed less than $5\ \mu\text{m}$ lateral displacement in any direction during the entire recording interval were categorized as static. An organelle often exhibits changes in speed and/or direction during the recording interval, sometimes separated by with pauses. Thus multiple “motile events” can be distinguished for a single organelle. Average speeds and run lengths were determined for all retrograde and anterograde “motile events” over $2\ \mu\text{m}$ using the kymographs.

Colocalization analysis

Colocalization was measured within biologically relevant regions of interest (ROIs) using ImageJ software to threshold images following the methods of Aiga *et al.*, (2011) and Brigidi *et al.* (2015). For a given marker (LAMP1, PI4KII α , GFP-Rab5, AP-3, EEA1, Rab7, DIC, mCh-Caly-WT, and mCh-Caly-ATEA), the same threshold value was applied to every image from a single experiment. ROIs consisted of thresholded fluorescence clusters with diameters $>0.3\ \mu\text{m}$. Colocalization was defined using the ImageJ Colocalization plug-in as areas of overlapping fluorescence within ROIs >4 pixels in size and with fluorescence intensity values exceeding threshold in both channels. A colocalization ratio was calculated by dividing the number of overlapping areas by the total number of ROIs stained by the marker of interest. The ImageJ plug-in Coloc2 was used to determine marker overlap in triple-stained images. A Manders tM2 was calculated for thresholded AP-3 and Caly signals using DIC image as mask. In COS7 cells, the number of vesicles was determined using the LoG detector function within ImageJ plug-in TrackMate v3.7.0, with the estimated blob diameter set to $0.15\ \mu\text{m}$ for EEs and to $0.3\ \mu\text{m}$ for LE/LROs.

Experimental design and statistical analysis

Experimental results are presented as the average obtained in at least three independent replicates, each involving neurons prepared from different animals. At least five different axons were analyzed per replicate. Grouped data were compared by *t* test or one-way analysis of variance followed by Dunnett’s posttest using GraphPad Prism 5 ($*p < 0.05$, $**p < 0.01$, $***p < 0.001$). Bar graphs show the mean and SEM of all calculated values; box-and-whisker plots show the mean, range (minimum to maximum), and 95% C.I. of the data.

ACKNOWLEDGMENTS

We are grateful to Victor Faundez and Stephanie Zlatić (Emory University) for EGFP-PI4KII plasmid DNA and Stephen King (University of Central Florida) for purified brain dynein. This work was supported by National Institutes of Health grants R01NS056314 (D.S.) and R21MH109280 (C.B.).

REFERENCES

- Aiga M, Levinson JN, Bamji SX (2011). N-cadherin and neuroligins cooperate to regulate synapse formation in hippocampal cultures. *J Biol Chem* 286, 851–858.
- Asensio CS, Sirkis DW, Edwards RH (2010). RNAi screen identifies a role for adaptor protein AP-3 in sorting to the regulated secretory pathway. *J Cell Biol* 191, 1173–1187.
- Bai J, He F, Novikova SI, Undie AS, Dracheva S, Haroutunian V, Lidow MS (2004). Abnormalities in the dopamine system in schizophrenia may lie in altered levels of dopamine receptor-interacting proteins. *Biol Psychiatry* 56, 427–440.
- Baracska KL, Haroutunian V, Meador-Woodruff JH (2006). Dopamine receptor signaling molecules are altered in elderly schizophrenic cortex. *Synapse* 60, 271–279.
- Barlan K, Gelfand VI (2017). Microtubule-based transport and the distribution, tethering, and organization of organelles. *Cold Spring Harb Perspect Biol* 9, a025817.
- Bely V, Schlager MA, Foster H, Reimer AE, Carter AP, Yildiz A (2016). The mammalian dynein-dynactin complex is a strong opponent to kinesin in a tug-of-war competition. *Nat Cell Biol* 18, 1018–1024.
- Bonifacino JS (2014). Adaptor proteins involved in polarized sorting. *J Cell Biol* 204, 7–17.
- Bonifacino JS, Traub LM (2003). Signals for sorting of transmembrane proteins to endosomes and lysosomes. *Annu Rev Biochem* 72, 395–447.
- Brigidi GS, Santyr B, Shimell J, Jovellar B, Bamji SX (2015). Activity-regulated trafficking of the palmitoyl-acyl transferase DHHC5. *Nat Commun* 6, 8200.
- Cai Q, Lu L, Tian J-H, Zhu Y-B, Qiao H, Sheng Z-H (2010). Snapin-regulated late endosomal transport is critical for efficient autophagy-lysosomal function in neurons. *Neuron* 68, 73–86.
- Carter AP, Diamant AG, Urnavicius L (2016). How dynein and dynactin transport cargos: a structural perspective. *Curr Opin Struct Biol* 37, 62–70.
- Clark RH, Stinchcombe JC, Day A, Blott E, Booth S, Bossi G, Hamblin T, Davies EG, Griffiths GM (2003). Adaptor protein 3-dependent microtubule-mediated movement of lytic granules to the immunological synapse. *Nat Immunol* 4, 1111–1120.
- Clinton SM, Ibrahim HM, Frey KA, Davis KL, Haroutunian V, Meador-Woodruff JH (2005). Dopaminergic abnormalities in select thalamic nuclei in schizophrenia: involvement of the intracellular signal integrating proteins calcyon and spinophilin. *Am J Psychiatry* 162, 1859–1871.
- Craige B, Salazar G, Faundez V (2008). Phosphatidylinositol-4-kinase type II α contains an AP-3-sorting motif and a kinase domain that are both required for endosome traffic. *Mol Biol Cell* 19, 1415–1426.
- Dai C, Liang D, Li H, Sasaki M, Dawson TM, Dawson VL (2010). Functional identification of neuroprotective molecules. *PLoS One* 5, e15008.
- Danglot L, Galli T (2007). What is the function of neuronal AP-3? *Biol Cell Auspices Eur Cell Biol Organ* 99, 349–361.
- Delevoe C, Heiligenstein X, Ripoll L, Gilles-Marsens F, Dennis MK, Linares RA, Derman L, Gokhale A, Morel E, Faundez V, *et al.* (2016). BLOC-1 brings together the actin and microtubule cytoskeletons to generate recycling endosomes. *Curr Biol* 26, 1–13.
- Delevoe C, Hurbain I, Tenza D, Sibarita J-B, Uzan-Gafsou S, Ohno H, Geerts WJC, Verkleij AJ, Salamero J, Marks MS, *et al.* (2009). AP-1 and KIF13A coordinate endosomal sorting and positioning during melanosome biogenesis. *J Cell Biol* 187, 247–264.
- Delevoe C, Miserey-Lenkei S, Montagnac G, Gilles-Marsens F, Paul-Gilloteaux P, Giordano F, Waharte F, Marks MS, Goud B, Raposo G (2014). Recycling endosome tubule morphogenesis from sorting endosomes requires the kinesin motor KIF13A. *Cell Rep* 6, 445–454.
- Driskell OJ, Mironov A, Allan VJ, Woodman PG (2007). Dynein is required for receptor sorting and the morphogenesis of early endosomes. *Nat Cell Biol* 9, 113–120.
- Encalada SE, Goldstein LSB (2014). Biophysical challenges to axonal transport: motor-cargo deficiencies and neurodegeneration. *Annu Rev Biophys* 43, 141–169.
- Evstratova A, Chamberland S, Faundez V, Tóth K (2014). Vesicles derived via AP-3-dependent recycling contribute to asynchronous release and influence information transfer. *Nat Commun* 5, 5530.
- Farrer MJ, Hulihan MM, Kachergus JM, Dächsel JC, Stoessl AJ, Grantier LL, Calne S, Calne DB, Lechevalier B, Chapon F, *et al.* (2009). DCTN1 mutations in Perry syndrome. *Nat Genet* 41, 163–165.

- Fu M, Holzbaur ELF (2014). Integrated regulation of motor-driven organelle transport by scaffolding proteins. *Trends Cell Biol* 24, 564–574.
- Ghiani CA, Starcevic M, Rodriguez-Fernandez IA, Nazarian R, Cheli VT, Chan LN, Malvar JS, de Vellis J, Sabatti C, Dell'Angelica EC (2010). The dysbindin-containing complex (BLOC-1) in brain: developmental regulation, interaction with SNARE proteins and role in neurite outgrowth. *Mol Psychiatr* 15, 115, 204–215.
- Grabner CP, Price SD, Lysakowski A, Cahill AL, Fox AP (2006). Regulation of large dense-core vesicle volume and neurotransmitter content mediated by adaptor protein 3. *Proc Natl Acad Sci USA* 103, 10035–10040.
- Harrison RE, Bucci C, Vieira OV, Schroer TA, Grinstein S (2003). Phagosomes fuse with late endosomes and/or lysosomes by extension of membrane protrusions along microtubules: role of Rab7 and RILP. *Mol Cell Biol* 23, 6494–6506.
- Hinckelmann M-V, Zala D, Saudou F (2013). Releasing the brake: restoring fast axonal transport in neurodegenerative disorders. *Trends Cell Biol* 23, 634–643.
- Hirst J, Barlow LD, Francisco GC, Sahlender DA, Seaman MNJ, Dacks JB, Robinson MS (2011). The fifth adaptor protein complex. *PLoS Biol* 9, e1001170.
- Hoang HT, Schlager MA, Carter AP, Bullock SL (2017). DYNC1H1 mutations associated with neurological diseases compromise processivity of dynein-dynactin-cargo adaptor complexes. *Proc Natl Acad Sci USA* 114, E1597–E1606.
- Ivan V, Martinez-Sanchez E, Sima LE, Oorschot V, Klumperman J, Petrescu SM, van der Sluijs P (2012). AP-3 and Rabip4' coordinately regulate spatial distribution of lysosomes. *PLoS One* 7, e48142.
- Jentsch JD, Trantham-Davidson H, Jairl C, Tinsley M, Cannon TD, Lavin A (2009). Dysbindin modulates prefrontal cortical glutamatergic circuits and working memory function in mice. *Neuropsychopharmacol Off Publ Am Coll Neuropsychopharmacol* 34, 2601–2608.
- King SJ, Schroer TA (2000). Dynactin increases the processivity of the cytoplasmic dynein motor. *Nat Cell Biol* 2, 20–24.
- Koh PO, Bergson C, Undie AS, Goldman-Rakic PS, Lidow MS (2003). Up-regulation of the D1 dopamine receptor-interacting protein, calcyon, in patients with schizophrenia. *Arch Gen Psychiatry* 60, 311–319.
- Larimore J, Tornieri K, Ryder PV, Gokhale A, Zlatic SA, Craige B, Lee JD, Talbot K, Pare J-F, Smith Y, et al. (2011). The schizophrenia susceptibility factor dysbindin and its associated complex sort cargoes from cell bodies to the synapse. *Mol Biol Cell* 22, 4854–4867.
- Laurin N, Misener VL, Crosbie J, Ickowicz A, Pathare T, Roberts W, Malone M, Tannock R, Schachar R, Kennedy JL, et al. (2005). Association of the calcyon gene (DRD11P) with attention deficit/hyperactivity disorder. *Mol Psychiatry* 10, 1117–1125.
- Lipka J, Kuijpers M, Jaworski J, Hoogenraad CC (2013). Mutations in cytoplasmic dynein and its regulators cause malformations of cortical development and neurodegenerative diseases. *Biochem Soc Trans* 41, 1605–1612.
- Lorenzo DN, Badea A, Davis J, Hostettler J, He J, Zhong G, Zhuang X, Bennett V (2014). A PIK3C3-ankyrin-B-dynactin pathway promotes axonal growth and multiorganelle transport. *J Cell Biol* 207, 735–752.
- Maday S, Twelvetrees AE, Moughamian AJ, Holzbaur ELF (2014). Axonal transport: cargo-specific mechanisms of motility and regulation. *Neuron* 84, 292–309.
- Maritzen T, Haucke V (2010). Gadkin: A novel link between endosomal vesicles and microtubule tracks. *Commun Integr Biol* 3, 299–302.
- Müller MJ, Klumpp S, Lipowsky R (2008). Tug-of-war as a cooperative mechanism for bidirectional cargo transport by molecular motors. *Proc Natl Acad Sci USA* 105, 4609–4614.
- Mullin AP, Gokhale A, Larimore J, Faundez V (2011). Cell biology of the BLOC-1 complex subunit dysbindin, a schizophrenia susceptibility gene. *Mol Neurobiol* 44, 53–64.
- Mullin AP, Sadanandappa MK, Ma W, Dickman DK, VijayRaghavan K, Ramaswami M, Sanyal S, Faundez V (2015). Gene dosage in the dysbindin schizophrenia susceptibility network differentially affect synaptic function and plasticity. *J Neurosci Off J Soc Neurosci* 35, 325–338.
- Muresan V, Muresan Z (2012). Unconventional functions of microtubule motors. *Arch Biochem Biophys* 520, 17–29.
- Muthusamy N, Faundez V, Bergson C (2012). Calcyon, a mammalian specific NEEP21 family member, interacts with adaptor protein complex 3 (AP-3) and regulates targeting of AP-3 cargoes. *J Neurochem* 123, 60–72.
- Neveling K, Martinez-Carrera LA, Hölker I, Heister A, Verrips A, Hosseini-Barkoie SM, Gilissen C, Vermeer S, Pennings M, Meijer R, et al. (2013). Mutations in BICD2, which encodes a golgin and important motor adaptor, cause congenital autosomal-dominant spinal muscular atrophy. *Am J Hum Genet* 92, 946–954.
- Newell-Litwa K, Seong E, Burmeister M, Faundez V (2007). Neuronal and non-neuronal functions of the AP-3 sorting machinery. *J Cell Sci* 120, 531–541.
- Oakman SA, Meador-Woodruff JH (2004). Calcyon transcript expression in macaque brain. *J Comp Neurol* 468, 264–276.
- Olenick MA, Tokito M, Boczkowska M, Dominguez R, Holzbaur ELF (2016). Hook adaptors induce unidirectional processive motility by enhancing the dynein-dynactin interaction. *J Biol Chem* 291, 18239–18251.
- Pandey JP, Smith DS (2011). A Cdk5-dependent switch regulates Lis1/Ndel1/dynein-driven organelle transport in adult axons. *J Neurosci Off J Soc Neurosci* 31, 17207–17219.
- Peden AA, Oorschot V, Hesser BA, Austin CD, Scheller RH, Klumperman J (2004). Localization of the AP-3 adaptor complex defines a novel endosomal exit site for lysosomal membrane proteins. *J Cell Biol* 164, 1065–1076.
- Peeters K, Litvinenko I, Asselbergh B, Almeida-Souza L, Chamova T, Geuens T, Ydens E, Zimo M, Irobi J, De Vriendt E, et al. (2013). Molecular defects in the motor adaptor BICD2 cause proximal spinal muscular atrophy with autosomal-dominant inheritance. *Am J Hum Genet* 92, 955–964.
- Puls I, Jonnakuty C, LaMonte BH, Holzbaur ELF, Tokito M, Mann E, Floeter MK, Bidus K, Drayna D, Oh SJ, et al. (2003). Mutant dynactin in motor neuron disease. *Nat Genet* 33, 455–456.
- Robinson JW, Leshchynska I, Farghaian H, Hughes WE, Sytryk V, Neely GG, Cole AR (2014). PI4KII α phosphorylation by GSK3 directs vesicular trafficking to lysosomes. *Biochem J* 464, 145–156.
- Salazar G, Love R, Werner E, Doucette MM, Cheng S, Levey A, Faundez V (2004). The zinc transporter ZnT3 interacts with AP-3 and it is preferentially targeted to a distinct synaptic vesicle subpopulation. *Mol Biol Cell* 15, 575–587.
- Salazar G, Zlatic S, Craige B, Peden AA, Pohl J, Faundez V (2009). Hermansky-Pudlak syndrome protein complexes associate with phosphatidylinositol 4-kinase type II alpha in neuronal and non-neuronal cells. *J Biol Chem* 284, 1790–1802.
- Scheuber A, Rudge R, Danglot L, Raposo G, Binz T, Poncer J-C, Galli T (2006). Loss of AP-3 function affects spontaneous and evoked release at hippocampal mossy fiber synapses. *Proc Natl Acad Sci USA* 103, 16562–16567.
- Schlager MA, Serra-Marques A, Grigoriev I, Gumy LF, Esteves da Silva M, Wulf PS, Akhmanova A, Hoogenraad CC (2014). Bicaudal d family adaptor proteins control the velocity of dynein-based movements. *Cell Rep* 8, 1248–1256.
- Schmidt MR, Maritzen T, Kukhtina V, Higman VA, Doglio L, Barak NN, Strauss H, Oschkinat H, Dotti CG, Haucke V (2009). Regulation of endosomal membrane traffic by a Gadkin/AP-1/kinesin KIF5 complex. *Proc Natl Acad Sci USA* 106, 15344–15349.
- Schreijer AMA, Fon EA, McPherson PS (2016). Endocytic membrane trafficking and neurodegenerative disease. *Cell Mol Life Sci* 73, 1529–1545.
- Schroeder CM, Vale RD (2016). Assembly and activation of dynein-dynactin by the cargo adaptor protein Hook3. *J Cell Biol* 214, 309–318.
- Seong E, Wainer BH, Hughes ED, Saunders TL, Burmeister M, Faundez V (2005). Genetic analysis of the neuronal and ubiquitous AP-3 adaptor complexes reveals divergent functions in brain. *Mol Biol Cell* 16, 128–140.
- Shi L, Muthusamy N, Smith D, Bergson C (2017). Dynein binds and stimulates axonal motility of the endosome adaptor and NEEP21 family member, calcyon. *Int J Biochem Cell Biol* 90, 93–102.
- Sirkis DW, Edwards RH, Asensio CS (2013). Widespread dysregulation of peptide hormone release in mice lacking adaptor protein AP-3. *PLoS Genet* 9, e1003812.
- Smith DS, Nithammer M, Ayala R, Zhou Y, Gambello MJ, Wynshaw-Boris A, Tsai LH (2000). Regulation of cytoplasmic dynein behaviour and microtubule organization by mammalian Lis1. *Nat Cell Biol* 2, 767–775.
- Smith DS, Skene JH (1997). A transcription-dependent switch controls competence of adult neurons for distinct modes of axon growth. *J Neurosci Off J Soc Neurosci* 17, 646–658.
- Talbot K, Cho D-S, Ong W-Y, Benson MA, Han L-Y, Kazi HA, Kamins J, Hahn C-G, Blake DJ, Arnold SE (2006). Dysbindin-1 is a synaptic and microtubular protein that binds brain snapin. *Hum Mol Genet* 15, 3041–3054.

- Taneichi-Kuroda S, Taya S, Hikita T, Fujino Y, Kaibuchi K (2009). Direct interaction of Dysbindin with the AP-3 complex via its mu subunit. *Neurochem Int* 54, 431–438.
- Twelvetrees AE, Pernigo S, Sanger A, Guedes-Dias P, Schiavo G, Steiner RA, Dodding MP, Holzbaur ELF (2016). The dynamic localization of cytoplasmic dynein in neurons is driven by kinesin-1. *Neuron* 90, 1000–1015.
- Voglmaier SM, Kam K, Yang H, Fortin DL, Hua Z, Nicoll RA, Edwards RH (2006). Distinct endocytic pathways control the rate and extent of synaptic vesicle protein recycling. *Neuron* 51, 71–84.
- Yamada M, Toba S, Yoshida Y, Haratani K, Mori D, Yano Y, Mimori-Kiyosue Y, Nakamura T, Itoh K, Fushiki S, et al. (2008). LIS1 and NDEL1 coordinate the plus-end-directed transport of cytoplasmic dynein. *EMBO J* 27, 2471–2483.
- Yap CC, Wisco D, Kujala P, Lasiecka ZM, Cannon JT, Chang MC, Hirling H, Klumperman J, Winckler B (2008). The somatodendritic endosomal regulator NEEP21 facilitates axonal targeting of L1/NgCAM. *J Cell Biol* 180, 827–842.
- Zelenin S, Aperia A, Diaz HR (2002). Calcyon in the rat brain: cloning of cDNA and expression of mRNA. *J Comp Neurol* 446, 37–45.